Intermetallics 28 (2012) 84–91

Contents lists available at SciVerse ScienceDirect

Intermetallics

journal homepage: www.elsevier.com/locate/intermet

Phase equilibria and structural investigations in the Ni-poor part of the system Al–Ge–Ni

Thomas L. Reichmann [a], Liliana I. Duarte [b], Herta S. Effenberger [c], Christian Leinenbach [b], Klaus W. Richter [a,*]

[a] University of Vienna, Department of Inorganic Chemistry/Materials Chemistry, Währingerstraße 42, 1090 Wien, Austria
[b] EMPA, Swiss Federal Laboratories for Materials Science and Technology, Laboratory for Joining and Interface Technology, Überlandstrasse 129, CH-8600 Dübendorf, Switzerland
[c] University of Vienna, Institute of Mineralogy and Crystallography, Althanstrasse 14, UZA II, A-1090 Wien, Austria

ARTICLE INFO

Article history:
Received 20 February 2012
Received in revised form
30 March 2012
Accepted 10 April 2012
Available online 8 May 2012

Keywords:
A. Nickel aluminides
A. Ternary alloy systems
B. Phase diagrams
B. Phase identification
B. Crystallography

ABSTRACT

The ternary phase diagram Al–Ge–Ni was investigated between 0 and 50 at.% Ni by a combination of differential thermal analysis (DTA), powder- and single-crystal X-ray diffraction (XRD), metallography and electron probe microanalysis (EPMA). Ternary phase equilibria and accurate phase compositions of the equilibrium phases were determined within two partial isothermal sections at 400 and 700 °C, respectively. The two binary intermediate phases AlNi and Al_3Ni_2 were found to form extended solid solutions with Ge in the ternary. Three new ternary phases were found to exist in the Ni-poor part of the phase diagram which were designated as τ_1 (oC24, $CoGe_2$-type), τ_2 (at approximately $Al_{67.5}Ge_{18.0}Ni_{14.5}$) and τ_3 (cF12, CaF_2-type). The ternary phases show only small homogeneity ranges. While τ_1 was investigated by single crystal X-ray diffraction, τ_2 and τ_3 were identified from their powder diffraction pattern.

Ternary phase reactions and melting behaviour were studied by means of DTA. A total number of eleven invariant reactions could be derived from these data, which are one ternary eutectic reaction, six transition reactions, three ternary peritectic reactions and one maximum. Based on the measured DTA values three vertical sections at 10, 20 and 35 at.% Ni were constructed. Additionally, all experimental results were combined to a ternary reaction scheme (Scheil diagram) and a liquidus surface projection.

1. Introduction

During the last several decades, aluminides of transition metals have been under investigation due to their excellent properties at high temperatures. Nickel aluminides are among the most commonly used intermetallics, in particular in terms of nickel-base superalloys. The major advantages of nickel-base superalloys are their excellent mechanical properties, such as good tensile and compressive yield strengths at high temperatures supplemented by a high creep strength [1]. These complex alloys are applied e.g. in turbine blades of aircraft and space vehicle engines, power generating gas turbines and marine propulsion turbines, respectively, where materials are subjected to elevated temperatures [2,3].

Since nickel-base superalloys are moulded at elevated temperatures in complex and cost-intensive procedures, a successful application of these materials requires suitable and cost-effective joining techniques. In this case diffusion brazing, also called transient liquid phase (TLP) joining [4], was successfully applied on nickel-base superalloys [5–7]. The respective brazing materials ideally provide definitely lower melting points than the substrates and possess similarities with respect to the chemical composition of the substrate. Germanium is a good candidate as a melting point depressant element of nickel aluminides, as it forms significant eutectics with Al and Ni [8]. For a better understanding of interface reactions and the phases occurring in the joint area, the detailed knowledge of the ternary phase diagram Al–Ge–Ni is essential.

The binary phase diagram Al–Ge is a simple eutectic system comprising limited solid solutions of Al and Ge. It has been recently re-evaluated by Srikanth et al. [9], based on earlier results of Minamino et al. [10] (who employed electron probe microanalysis), and McAlister and Murray [11]. According to Minamino et al, the eutectic reaction temperature is 696.85 K with the eutectic composition $Al_{72.0}Ge_{28.0}$.

A detailed evaluation of the Al–Ni phase diagram was given by Nash et al. [12]. The following intermediate compounds have been found to exist in the system: Al_3Ni, Al_3Ni_2, AlNi, $AlNi_3$ and Al_3Ni_5. The phases Al_3Ni, Al_3Ni_2 and $AlNi_3$ are formed peritectically

* Corresponding author. Tel.: +43 1 4277 52910; fax: +43 1 4277 9529.
E-mail address: klaus.richter@univie.ac.at (K.W. Richter).

0966-9795
doi:10.1016/j.intermet.2012.04.002

whereas AlNi is melting congruently at 1638 °C. This melting point was found to be much higher in more recent papers, e.g. Bitterlich et al. [13], who found the melting point of stoichiometric AlNi at 1681 °C. Al_3Ni_5 crystallizes through a solid–state reaction of AlNi and $AlNi_3$. An update of the Al–Ni system, which was consulted in the current work, was given by Okamoto [14].

The binary phase diagram Ge–Ni is rather complex, and is not completely established in the area between 25 and 50 at.% Ge where a multitude of phases were reported. In the composition range relevant for the current study, GeNi is the only intermetallic compound. It melts peritectically at 850 °C and shows a eutectic reaction with Ge at 762 °C and 67 at.% Ge. The system was assessed by Nash et al. [15] based on experimental results of Dayer and Feschotte [16] and Ellner et al. [17].

Although the binary limiting systems Al–Ge, Al–Ni and Ge–Ni are well investigated, only limited information is available for the ternary system Al–Ge–Ni. It was examined by Yanson et al. [18], who constructed an isothermal section at 770 K, using X-ray powder diffraction and optical microscopy. A ternary intermediate compound Σ, with the empirical formula $AlGeNi_4$, was reported without any additional structural information. Maximum solubilities of about 3.0 at.% Ge in the Al_3Ni_2 binary phase and 7.0 at.% Ge in AlNi were indicated. A continuous solid solution of the two phases $AlNi_3$ and $GeNi_3$ (both $L1_2$-structure) was determined by means of optical microscopy which was also shown by Ochiai et al. [19], who employed X-ray methods and metallography at 1273 K. No information on the ternary phase reactions and melting behaviour in the ternary system could be found in literature.

A list of crystallographic data of binary and ternary compounds relevant for the current work is given in Table 1 together with relevant citations [20–25].

In the current work we present a complete study of the Al–Ge–Ni phase diagram in the composition range between 0 and 50 at.% Ni. Phase equilibria in the Ni-rich part of the system are still under investigation and will be given separately.

2. Experimental

All samples were prepared from pure elements, using aluminium slug (99.999%, Johnson Matthey Chemicals), germanium pieces (99.999%, Johnson Matthey Chemicals) and nickel foil (99.99%, Advent Research Materials Ltd.). The compositions were weighed with a semi-micro balance to the accuracy of about ±0.5 mg and ±0.1 at.%, respectively. Arc furnace melting was performed under argon atmosphere, using zirconium as getter material. To guarantee a homogeneous distribution of the basic materials the reguli were turned and melted three times. They were weighed back to check for possible mass losses, and these were negligible in all samples.

For equilibration, the samples were placed into alumina crucibles, sealed into evacuated silica glass tubes and annealed at 400 and 700 °C, respectively, for at least three weeks. Two different methods were applied for annealing. On the one hand the reguli were directly sealed into silica glass and on the other hand they were powdered and pressed to pills before annealing, to allow for short diffusion paths. Due to the minor compactness of the pills, the latter method was not suitable to produce proper surface grindings, for subsequent metallographic investigation.

After quenching in cold water the samples were investigated by a combination of powder XRD, optical microscopy, scanning electron microscopy (SEM), electron probe microanalysis (EPMA) and differential thermal analysis (DTA).

For the investigations of the microstructures, the samples were embedded in phenolic hot mounting resin and then ground and polished. Grinding was performed with silicon carbide abrasive paper whereas for polishing abrasive corundum powder was used. Metallographic analyses were carried out on a binocular reflected-light microscope (Zeiss Axiotech 100) featured with a bi-refringent prism for differential interference contrast (DIC) imaging and equipment for operation under polarized light.

Quantitative examination of the microstructures was performed by a Cameca SX electron probe 100 (EPMA) equipped with four high sensitive diffracting crystals. Measurements were carried out with an acceleration voltage of 15 kV and a beam current of 10 nA using a wavelength dispersive X-ray detector (WDX). Pure aluminium, germanium and nickel were employed as standard materials. Conventional ZAF matrix correction was applied to calculate final compositions from the measured X-ray intensities. SEM measurements were done on a Zeiss Supra 55 VP environmental scanning electron microscope using pure cobalt for an energy calibration of the EDX detector signal. The composition of each phase was measured at three or more spots in order to minimize statistical errors and obtain more reliable results.

Phase identifications and precise lattice parameters of the different phases were obtained by means of X-ray powder diffraction (XRD) using a Bruker D8 Discover Series 2 powder diffractometer in Bragg-Brentano pseudo-focussing geometry (CuKα, LynxEye silicon strip detector). Additional measurements were performed on a Guinier-Huber camera 670 operating with $CuK\alpha_1$ radiation and an image plate detector (measurement period: 1 h, 10 detection loops). For XRD measurements small pieces of each sample were powdered with a tungsten carbide mortar. More ductile samples were powdered with a ball mill and afterwards stress annealed for about 15 min.

For crystal structure determination of the new ternary phases, a Nonius Kappa CCD diffractometer, equipped with a monocapillary optics collimator, graphite monochromatized MoKα radiation and a position sensitive planar X-ray detector, was applied. The structure refinement was done with the software SHELXL-97 [26].

DTA measurements were carried out on a Netzsch DTA 404 PC using open alumina crucibles and a constant argon flow of 50 mL/min, respectively. Titanium was used as getter material. The temperature was measured with type-S (Pt/Pt10%Rh) thermocouples which were calibrated at the melting points of pure Al, Au and Ni. The samples weighed usually around 100 mg and were located in good thermal contact to the crucibles. Two heating- and

Table 1
Crystal structure data of binary and ternary phases relevant for the present study.

Phases	Lattice parameter (Å)	Structure type	Space group	Reference
Al	$a = 4.0492$	Cu	*Fm-3m*	[20]
Al_3Ni	$a = 6.5982$, $b = 7.3515$, $c = 4.8021$	Fe_3C	*Pnma*	[21]
Al_3Ni_2	$a = 4.0363$, $c = 4.9004$	Al_3Ni_2	*P-3m1*	[21]
AlNi	$a = 2.848$	CsCl	*Pm-3m*	[22]
$AlNi_3$	$a = 3.608$	$AuCu_3$	*Pm-3m*	[23]
GeNi	$a = 5.381$, $b = 3.428$, $c = 5.811$	MnP	*Pnma*	[24]
Ge	$a = 5.656$	C	*Fd-3m*	[25]
$Al_xGe_{2-x}Ni$ (τ_1)	$a = 10.760$ (2), $b = 5.715$ (1), $c = 5.713$ (1)	$CoGe_2$	*Cmca*	this work
τ_2	$a = 11.4025$ (1)	–	*I-43m*	this work
$Al_xGe_{2-x}Ni$ (τ_3)	a = 5.6475(1)	CaF_2	*Fm-3m*	this work

cooling-curves were recorded for each sample using a heating rate of 5 K min^{-1}. After measuring the samples were re-weighed in order to check for possible mass losses during the experiment. No systematic mass losses were observed in this regard.

3. Results and discussion

A total number of 26 samples were prepared for the investigation of isothermal phase equilibria and occurring phase reactions within the investigated composition area. Two partial isothermal sections at 400 and 700 °C, respectively, and vertical sections at 10, 20 and 35 at.% Ni were derived from these samples. A partial reaction scheme and a liquidus projection was also constructed. Furthermore, as-cast samples were consulted for examinations of primary crystallization and a specific slow-cooling procedure was used for the generation of suitable single crystals of the new ternary compound τ_1.

3.1. Isothermal sections at 400 and 700 °C

An initial characterization of the samples annealed at 400 and 700 °C was done by means of powder XRD. Accurate phase compositions were further determined by EPMA and SEM. On the basis of the combined results two partial isothermal sections at 400 and 700 °C were drawn which show large differences to prior results of Yanson et al. [18]. The results for selected samples annealed at 400 and 700 °C are presented in Table 2. It is estimated, that the phase compositions measured are accurate within ±0.5 at.%. It is to mention that some samples, annealed at 400 °C, were not in equilibrium and contained traces of a fourth phase after annealing. These samples are explicitly marked in Table 2. Additional samples were thus prepared, which were powdered and pressed before annealing, in order to verify the interpretation of equilibrium phase relations. With this method it was possible to reduce the amount of the non-equilibrium phase in each sample.

In the partial isothermal section at 400 °C, given in Fig. 1, nine three-phase fields were experimentally determined: Al–Al_3Ni-τ_2, Al–Ge-τ_2, Al_3Ni–Ge-τ_2, Al_3Ni–(Al_3Ni_2)–Ge, (AlNi)–Ge-τ_3, Ge-τ_1-τ_3, (AlNi)-τ_1-τ_3, Ge–GeNi-τ_1; whereas one three-phase field (AlNi)–(Al_3Ni_2)–Ge was not measured with EPMA, but confirmed with powder XRD. No sample was placed in the area of the three phase field (AlNi)–GeNi- τ_1. The solid solubility of Ge in Al was found to be around 1.8 at.% at 400 °C, consistent with previous studies by Eslami et al. [27]. The limiting solubilities of Ge in Al_3Ni and of Al in GeNi were measured with EPMA to be approximately 0.4 at.% and 0.8 at.%, respectively. This is comparable to the solubilities for the respective phases found in Al–Ni–Si [28].

(Al_3Ni_2), however shows an extended solubility of about 14 at.% Ge. As to be expected, Al is partially replaced by Ge, so the Ni-content remains constant at 40 at.% in the entire homogeneity range. The corresponding variation in lattice parameters of (Al_3Ni_2) with raising Ge content was found to be a = 4.0363–4.0525 Å and c = 4.9004–4.8354 Å. Based on our results in the ternary, the homogeneity range of Al_3Ni_2 at 400 °C is significantly smaller than proposed by Okamoto [14].

The homogeneity range of (AlNi) turned out to be difficult to determine due to fluctuations of the EPMA results. Since AlNi melts congruently at around 1681 °C [13], solidification temperatures of ternary samples which primary crystallize (AlNi) are very high and the corresponding primary crystals are large. Thus, equilibration during annealing at 400 °C was not reached in every sample due to very long diffusion paths. We used samples containing only small amounts of (AlNi) for the determination of the solubility limit which was found to be approximately 5 at.%. The solubilities of Al and Ni in Ge determined in different samples showed also large fluctuations, and partly unrealistically high values. This may be connected with the formation of small Ni-precipitates in Ge formed on fast cooling after arc melting. Therefore we decided to rely on literature values for the binary systems, and did not include experimental values for Ge in Table 2.

Table 2
Experimental phase compositions and cell parameters of the selected samples annealed at 400 and 700 °C.

Sample/comp. (at.%)	Phase analysis			EPMA/ SEM		
	Annealing (°C)	Phase	XRD Lattice parameter (Å)	Al (at.%)	Ge (at.%)	Ni (at.%)
$Al_{75}Ge_{15}Ni_{10}$[a]	400	Al	a = 4.0511(1)	97.9	1.7	0.4
		Ge	a = 5.6605(1)	–	–	–
		τ_2	unknown structure	67.9	18.3	13.8
$Al_{75}Ge_5Ni_{20}$[a]	400	Al	a = 4.0509(1)	97.8	1.8	0.4
		Al_3Ni	a = 6.6167(1),	74.8	0.1	25.1
		τ_2	b = 7.3708(2),	67.5	17.2	15.3
			c = 4.8152(1)			
$Al_{65}Ge_{15}Ni_{20}$	400	Al_3Ni	unknown structure			
		Ge	a = 6.6165(1),	74.1	0.8	25.1
		τ_2	b = 7.3711(1),	–	–	–
			c = 4.8153(1)	67.0	17.8	15.2
$Al_{55}Ge_{25}Ni_{20}$[a]	400	Al_3Ni	a = 5.6608(1)			
		(Al_3Ni_2)	unknown structure			
		Ge	a = 6.6166(2),	74.6	0.2	25.2
			b = 7.3718(2),	57.1	2.9	40.0
			c = 4.8156(1)	–	–	–
$Al_{15}Ge_{65}Ni_{20}$[a]	400	Ge	a = 4.0408(1),			
		τ_1	c = 4.8806(1)			
		τ_3	a = 5.6617(1)			
$Al_{40}Ge_{25}Ni_{35}$	400	(Al_3Ni_2)	a = 5.6589(1)	–	–	–
		Ge	a = 10.7512(1),	17.7	48.9	33.4
		τ_3	b = 5.7056(8),	25.7	39.9	34.4
			c = 5.6990(8)			
$Al_{30}Ge_{35}Ni_{35}$	400	(AlNi)	a = 5.6495(1)			
		Ge	a = 4.0525(1),	46.6	13.7	39.8
		τ_3	c = 4.8354(1)	–	–	–
$Al_{20}Ge_{45}Ni_{35}$[a]	400	(AlNi)	a = 5.6572(1)			
		τ_1	a = 2.8872(1)	46.1	5.2	48.7
		τ_3	a = 5.6576(1)	–	–	–
			a = 5.6405(1)	26.8	38.2	35.0
$Al_{10}Ge_{55}Ni_{35}$	400	Ge	a = 2.8867(1)	45.6	5.4	49.0
		GeNi	a = 10.7534(2),	17.2	49.1	33.8
		τ_1	b = 5.7035(1),	24.8	40.5	34.7
			c = 5.6989(1)			
$Al_5Ge_{45}Ni_{50}$	700	(AlNi)	a = 5.5905(2)			
		GeNi	a = 5.3891(2),	0.8	49.2	50.0
		τ_1	b = 3.4381(1),	15.0	51.3	33.7
			c = 5.8173(2)			
$Al_{14}Ge_{45}Ni_{41}$	700	(AlNi)	a = 10.7575(2),			
		GeNi	b = 5.7128(1),			
		τ_1	c = 5.7075(1)			
$Al_9Ge_{65}Ni_{26}$	700	Ge	a = 2.8890(3)	42.2	8.3	49.6
		GeNi	a = 5.3904(1),	1.2	48.7	50.1
		τ_1	b = 3.4372(1),			
			c = 5.8172(1)			
			a = 2.8865(1)	43.8	9.0	47.3
			a = 5.3886(2),	1.2	48.8	50.0
			b = 3.4383(1),	16.4	49.6	34.1
			c = 5.8148(2)			
			a = 10.7559(4),			
			b = 5.7103(3),			
			c = 5.7043(3)			
			a = 5.6592(1)	–	–	–
			a = 5.3849(1),	0.8	49.8	49.4
			b = 3.4409(6),	14.7	52.4	32.9
			c = 5.8112(1)			
			a = 10.7619(4),			
			b = 5.7165(3),			
			c = 5.7090(3)			

[a] Traces of an additional phase present.

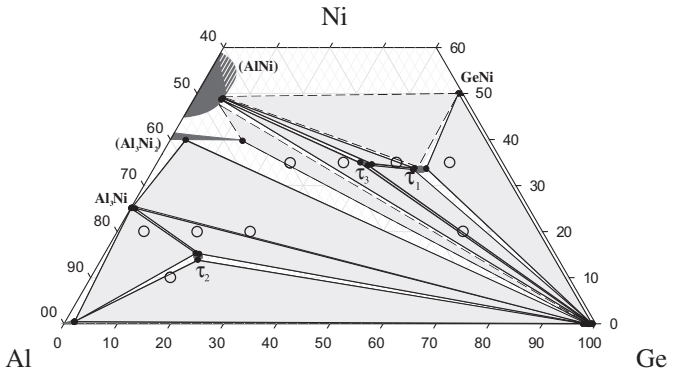

Fig. 1. Partial isothermal section at 400 °C. Large circles: nominal compositions of the respective samples. Small circles: measured phase compositions with EPMA or SEM.

In addition to the binary phases discussed above, three new ternary compounds have been found to exist in the isothermal section at 400 °C. All phases were found to be stable within small composition ranges around $Al_{15.0}Ge_{51.5}Ni_{33.5}$ (τ_1), $Al_{67.5}Ge_{18.0}Ni_{14.5}$ (τ_2) and $Al_{25.5}Ge_{40.0}Ni_{34.5}$ (τ_3). τ_1 and τ_3 were also found in the isothermal section at 700 °C. The homogeneity range of τ_1 was also well defined by EPMA and shown in the partial isothermal section at 700 °C (Fig. 2).

The isothermal section at 700 °C includes several three-phase equilibria which were not all determined experimentally, but partly extrapolated form the isothermal section at 400 °C: L–Al_3Ni–(Al_3Ni_2), L–(Al_3Ni_2)–Ge, (AlNi)–(Al_3Ni_2)–Ge, (AlNi)–Ge-τ_3, Ge-τ_1-τ_3, (AlNi)-τ_1-τ_3, Ge–GeNi-τ_3, (AlNi)–GeNi-τ_3.

As for 400 °C, it was also difficult to determine reliable solubility of Ge in (AlNi) at 700 °C. Therefore, four samples with the nominal compositions $Al_{45}Ge_5Ni_{50}$, $Al_{30}Ge_{20}Ni_{50}$, $Al_{17}Ge_{33}Ni_{50}$ and $Al_5Ge_{45}Ni_{50}$, which were all lying on the same tie-line between (AlNi) and GeNi, were consulted to investigate the solubility of Ge in (AlNi) at 700 °C. The respective solubilities (3.6–7.6 at.%), measured with EPMA, were found to be in a linear correlation (Vegard's rule) with the corresponding lattice parameters (2.8872–2.8890 Å). The plot is given in Fig. 3. One additional sample was produced at $Al_{40}Ge_{10}Ni_{50}$. To guarantee for equilibrium within this sample, it was powdered and further pressed to a pill, before it was annealed for 2 months at 700 °C. As it was not possible to determine phase compositions with EPMA directly (due to the bad compactness of the pill), the composition of (AlNi) was determined from the lattice parameters. It was refined with $a = 2.8893(1)$ Å which leads to a calculated Ge solubility of approximately 8 at.% at 700 °C. The calculated Ge content is

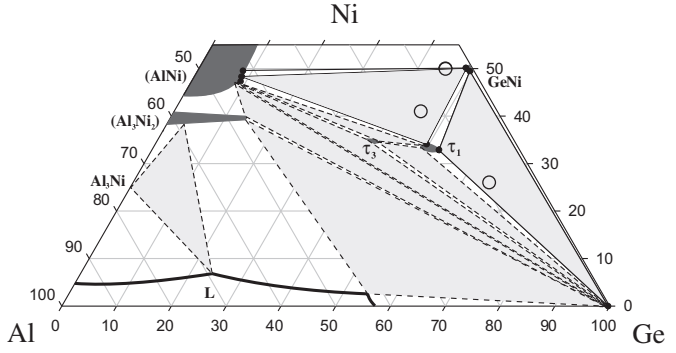

Fig. 2. Partial isothermal section at 700 °C. Large circles: nominal compositions of the respective samples. Small circles: phase compositions measured with EPMA.

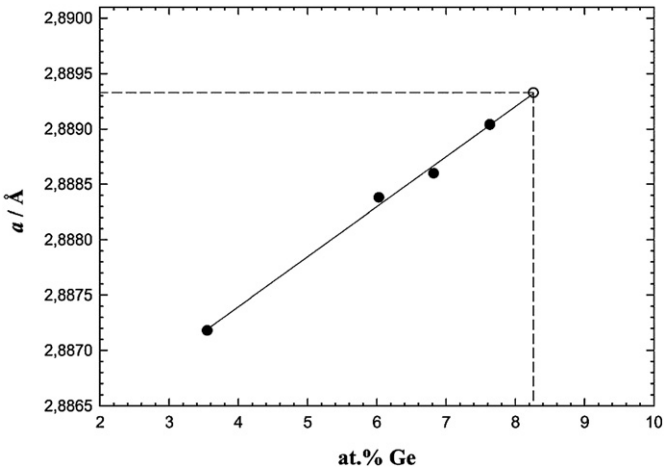

Fig. 3. Lattice parameter a shown as a function of Ge content in (AlNi). Open circle: sample at $Al_{40}Ge_{10}Ni_{50}$ equilibrated in form of a pressed pill. Full circles: bulk samples; composition measured with EPMA.

comparable to the value of a sample at $Al_{14}Ge_{45}Ni_{41}$, which was determined to be 9.0 at.%. The latter sample is located on a tie-triangle which enters (AlNi) close to the tie-line of (AlNi)–GeNi.

3.2. Synthesis and crystal structure of the compound $Al_xGe_{2-x}Ni$ ($x \approx 0.5$) (τ_1)

τ_1 was determined with EPMA to be stable within the composition range of $Al_{14.5}Ge_{52.8}Ni_{32.7}$ to $Al_{17.2}Ge_{49.1}Ni_{33.7}$ at 700 °C. A sample with the nominal composition $Al_{16}Ge_{51}Ni_{33}$ was produced for generating a pure powder pattern of τ_1. Indexing of this powder pattern led to an orthorhombic unit cell. The attempt to extract single crystals of τ_1 was not successful due to a fine and typical peritectic microstructure. DTA measurements led to an invariant reaction temperature of 809 ± 1 °C. Based on the primary crystallisation field of τ_1 (see Section 3.5.), a sample with the nominal composition $Al_6Ge_{63}Ni_{31}$ was slowly cooled from 829 to 700 °C in order to produce single crystals of τ_1. The corresponding microstructure, shown in Fig. 4, exhibited τ_1 as primary crystallised phase. A suitable single crystal with the dimensions 0.02 × 0.02 × 0.10 mm was extracted from the sample. Single

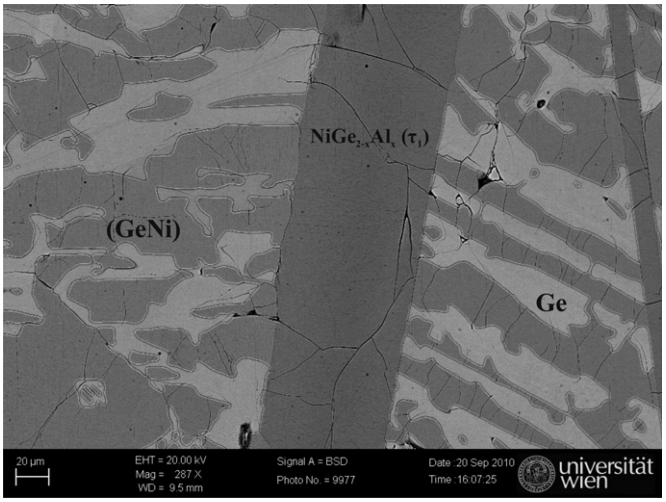

Fig. 4. BSE image of a slowly cooled sample with the nominal composition $Al_6Ge_{63}Ni_{31}$, showing τ_1 as primary crystals.

Table 3
Selected data collection and refinement parameters for $Al_xGe_{2-x}Ni$ (τ_1).

Empirical formula	$Al_{0.44}$ $Ge_{1.56}Ni_1$
Crystal system, space group	Orthorhombic, *Cmca*
Cell dimensions	
a/Å	10.760 (2)
b/Å	5.715 (1)
c/Å	5.713 (1)
V/Å^3	351.310 (1)
ρ_{calc}/g cm^{-3}; $\mu(MoK\alpha)$/mm^{-1}	5.985; 27.73
Z	8
Crystal size/ mm^3	0.02 × 0.02 × 0.1
Detector- sample distance/mm	30
Number of images; rotation angle per image/°	539; 2
Scan time/ s/°; frame size/pixels	100; 621 × 576
Total reflections	2210
Unique reflections (n); reflections with $F_o > 4\sigma(F_o)$	405; 377
$R_{int} = \Sigma\lvert F_o^2 - F_o^2(mean)\rvert/\Sigma F_o^2$	0.0582
$R1 = \Sigma(\lvert\lvert F_o\rvert - \lvert F_c\rvert\rvert)/\Sigma\lvert F_o\rvert$	0.0234
$wR^2 = [\Sigma w(F_o^2 - F_c^2)^2/\Sigma wF_o^4]^{1/2}$	0.0555
$GooF = [\Sigma w(F_o^2 - F_c^2)^2/(n-p)]^{1/2}$	1.169
Extinction parameter	0.0049(6)
Max Δ/σ; number of variable parameters (p)	<0.001; 20
Final difference Fourier map/eÅ^{-3}	0.29

Table 4
Atomic coordinates and equivalent isotropic displacement parameters for $Al_xGe_{2-x}Ni$ (τ_1).

Atomic position	Wykoff letter	Occupation	x	y	z	U_{eq}
Ni	8(d)	1.0	0.11656 (4)	0	0	0.0092 (1)
M1	8(f)	0.96 (1) Ge+ 0.04 (1) Al	0	0.15432 (6)	0.34454 (6)	0.0097 (1)
M2	8(e)	0.65 (1) Ge+ 0.35 (1) Al	0.25000	0.24831 (8)	0.25000	0.0100 (1)

Table 5
Anisotropic displacement parameters for $Al_xGe_{2-x}Ni$ (τ_1).

Atomic position	*U*11	*U*22	*U*33	*U*23	*U*13	*U*12
Ni	0.0077 (2)	0.0105 (2)	0.0095 (2)	0	0	0
M1	0.0116 (2)	0.0091 (2)	0.0086 (2)	0	0	0
M2	0.0089 (2)	0.0111 (2)	0.0101 (2)	0	0.0001 (1)	0

crystal XRD measurements were carried out at 30 mm crystal-detector distance and 2° rotation per frame. 539 frames in total were collected with an exposure time of 100 s per degree. Unit cell data as well as refinement parameters are given in Table 3. The ternary compound τ_1 was found to crystallize in the $CoGe_2$-type structure and was refined with a starting model using the structure data for high-pressure Ge_2Ni given by Takizawa et al. [29].

The structure of τ_1 consists of three atomic positions, where one is totally filled with Ni atoms and two are mixed positions of Al and Ge. Atomic positions, occupation factors and anisotropic displacement factors are listed in Tables 4 and 5. The chemical composition, calculated from the refinement ($Al_{14.7}Ge_{52.0}Ni_{33.3}$) is in excellent agreement with EPMA results ($Al_{14.4}Ge_{52.8}Ni_{32.8}$) and corresponds to the empirical formula $Al_{0.44}Ge_{1.56}Ni$. It is to mention that the latter compositions are both given for 700 °C. Phase stability of $Al_xGe_{2-x}Ni$ at 400 °C was measured within the range $x = 0.45–0.52$.

The $CoGe_2$ structure was already described in detail by Takizawa et al. [29]. The structure is known as to be an intermediate structure between the CaF_2- and the $CuAl_2$-type structure. The relation is due to similar atomic coordination within the three structure types. The cubic coordination, as it occurs in the CaF_2-type, is shifted to a square anti prism with one additional transition metal position ($CoGe_2$) and two additional transition metal positions ($CuAl_2$), respectively, in the first coordination sphere. The CaF_2 structure also exhibits the tetrahedral arrangement of the main group elements whereas the $CuAl_2$ structure maintains the rectangular pyramidal coordination. Both atom arrangements are also present in the $CoGe_2$ structure. For more details on the crystal structure we refer to Ref. [29]. Detailed structural information on τ_1 was deposited in Fachinformationszentrum Karlsruhe, 76344 Eggenstein-Leopoldshafen, Germany, (fax: (49) 7247 808 666; e-mail: crysdata@fiz.karlsruhe.de) and can be obtained on quoting the depository number CSD 424184.

3.3. A new ternary compound at $Al_{67.5}Ge_{18.0}Ni_{14.5}$ (τ_2)

The presence of a new ternary compound with a composition close to $Al_{67.5}Ge_{18.0}Ni_{14.5}$ was confirmed by XRD and EPMA. The corresponding limiting compositions of τ_2 are given in Table 2. The XRD pattern of a sample with the nominal composition $Al_{75}Ge_{15}Ni_{10}$ (shown in Fig. 5) was used for an indexing attempt

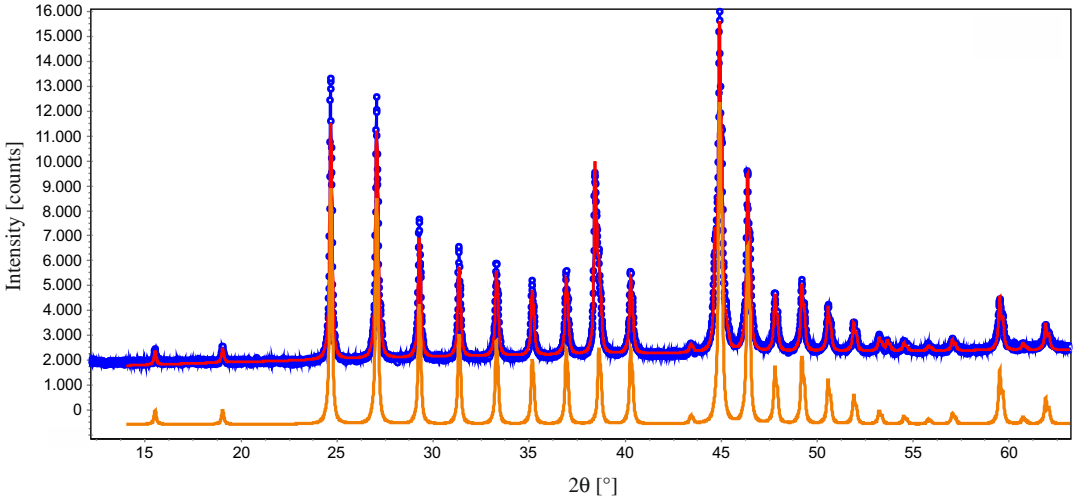

Fig. 5. Powder XRD pattern of a sample with the nominal composition $Al_{75}Ge_{15}Ni_{10}$ showing the pattern of τ_2 together with minor amounts of Al and Ge. Up: experimental (blue points) and refined (red line) pattern. Below: calculated pattern of cubic τ_2 (orange line). (For interpretation of the references to colour in this figure legend, the reader is referred to the web version of this article).

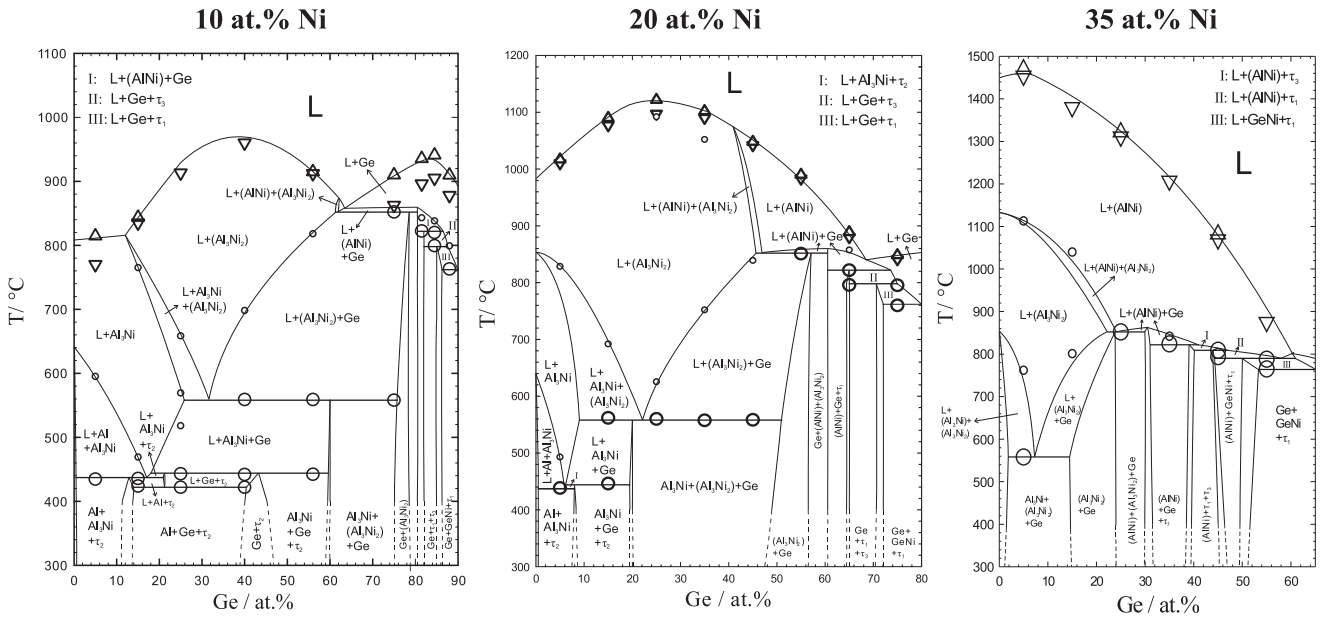

Fig. 6. Vertical sections at 10, 20 and 35 at.% Ni. Large circles: invariant thermal effects. Small circles: non-invariant effects. Triangles up: liquidus on heating. Triangles down: liquidus on cooling. Dotted lines: assumed phase boundaries.

Table 6
Ternary invariant reactions determined in the present study.

Reaction	T/ °C	Phase	Composition/at.%		
			Al	Ge	Ni
E1: L = Al + Ge + τ_2	423 ± 2	L	71.3	28.6	0.1
		Al	98.0	1.8	0.2
		Ge	1.0	99.0	0.0
		τ_2	67.5	18.5	14.0
U1: L + Al_3Ni = Al + τ_2	437 ± 2	L	71.5	27.5	1.0
		Al_3Ni	24.8	0.5	74.7
		Al	98.0	1.8	0.2
		τ_2	68.0	18.0	14.0
P1: L + Al_3Ni + Ge = τ_2	444 ± 2	L	70.5	28.5	1.0
		Al_3Ni	24.8	0.5	74.7
		Ge	1.0	99.0	0.0
		τ_2	68.0	17.5	14.5
U2: L + (Al_3Ni_2) = Al_3Ni + Ge	558 ± 2	L	59.0	40.0	1.0
		(Al_3Ni_2)	57.5	2.5	40.0
		Al_3Ni	24.8	0.5	74.7
		Ge	1.0	99.0	0.0
U3: L + (AlNi) = (Al_3Ni_2) + Ge	852 ± 2	L	28.0	63.0	9.0
		(AlNi)	46.5	6.5	47.0
		(Al_3Ni_2)	46.0	14.0	40.0
		Ge	0.6	99.4	0.0
Max1: L = (AlNi) + Ge	~860	L	14.8	68.2	17.0
		(AlNi)	46.5	6.5	47.0
		Ge	0.5	99.5	0.0
U4: L = Ge + GeNi + τ_1	763 ± 3	L	0.0	67.0	33.0
		Ge	0.7	99.3	0.0
		GeNi	0.5	50.0	49.5
		τ_1	13.2	53.8	33.0
U5: L + (AlNi) = GeNi + τ_1	790 ± 4	L	4.0	60.0	36.0
		(AlNi)	45.0	7.0	48.0
		GeNi	0.7	49.8	49.5
		τ_1	17.0	50.0	33.0
U6: L + τ_3 = Ge + τ_1	798 ± 3	L	6.3	66.7	27.0
		τ_3	25.5	40.0	34.5
		Ge	0.7	99.3	0.0
		τ_1	15.0	52.0	33.0
P2: L + τ_3 + (AlNi) = τ_1	809 ± 1	L	8.5	61.0	30.5
		τ_3	25.0	40.0	35.0
		(AlNi)	46.0	6.0	48.0
		τ_1	17.5	49.0	33.5
P3: L + (AlNi) + Ge = τ_3	822 ± 2	L	8.0	66.5	25.5
		(AlNi)	46.2	6.3	47.5
		Ge	0.8	99.2	0.0
		τ_3	25.5	40.0	34.5

with DIFFRAC^{plus} TOPAS software. As a proper solution a base-centered cubic cell arrangement with the approximate lattice parameter a = 11.04 Å was found.

The phase τ_2 was found to be in thermodynamic equilibrium with Al, Ge and Al_3Ni. It is formed peritectically by the reaction L + Al_3Ni + Ge = τ_2 at 444 ± 2 °C (compare Section 3.5). The determination of the crystal structure of τ_2 is currently in progress and it will be published separately.

3.4. Crystal structure of the compound $Al_xGe_{2-x}Ni$ ($x \approx 0.8$) (τ_3)

In the vicinity of τ_1 another ternary compound, designated as τ_3, was found to exist. A sample with the nominal composition $Al_{24.8}Ge_{40.5}Ni_{34.7}$ was investigated with powder XRD and EPMA. The sample was found to be located within a two-phase field τ_3-(AlNi). Unknown reflections were indexed, which yielded the best consistency for a cubic cell with face-centered Bravais lattice. The observed cell parameters suggested the well-known CaF_2-type structure as possible structural model. For refinement a mixed position of Al and Ge was assumed. Site occupation factors were calculated from the measured composition of τ_3 with 0.61 for Al and 0.39 for Ge. The refined lattice parameter is a = 5.6462(1) Å. τ_3, stoichiometrically described as $Al_xGe_{2-x}Ni$, is only stable within a small homogeneity range between $Al_{24.8}Ge_{40.5}Ni_{34.7}$ and $Al_{26.8}Ge_{38.2}Ni_{35.0}$ at 400 °C. The measured Ni content was found to be slightly higher than expected from the stoichiometric composition. More details on the crystal structure of τ_3 may be obtained from the Fachinformationszentrum Karlsruhe on quoting the depository number CSD 424185.

Phase relations of τ_3 are discussed in 3.5. An incongruent formation was assumed due to peritectic microstructures of samples containing τ_3. The corresponding peritectic reaction was assessed to be L+(AlNi)+Ge = τ_3 with the reaction temperature of approximately 822 ± 2 °C. The reaction temperature is close to the peritectic formation temperature of τ_1 which is at 809 ± 1 °C.

3.5. Ternary reactions and liquidus projection

Ternary phase reactions and reaction temperatures were studied by means of differential thermal analysis (DTA). Based on the experimental results, three vertical sections at constant Ni concentration of 10, 20 and 35 at.% were constructed to represent phase relations at variable temperatures. For each sample two heating- and cooling-cycles were performed at a rate of 5 K/min in order to check if equilibrium conditions can be restored on cooling with 5 K/min. It was found that most of the DTA samples, especially in the Ni poor part of the system, were not in equilibrium after the first cycle. All non-invariant as well as invariant effects, measured in the first heating curves, were taken for the graphical representations shown in Fig. 6. The liquidus values were calculated as mean values from both cycles. Although most of the cooling curves exhibited strong supercooling their liquidus values were also considered in Fig. 6.

The vertical sections were constructed by combining DTA results with phase boundaries obtained in the isothermal sections. Within the three vertical sections, eleven invariant reactions were found, including one degenerated eutectic, three ternary peritectics, six transition reactions and one maximum. The three ternary peritectic reactions P1, P2 and P3 correspond to the incongruent formations of τ_2, τ_1 and τ_3, respectively. All reactions, the averaged invariant reaction temperatures and estimated compositions of the involved phases at the respective reaction temperatures, are presented in Table 6.

In the very narrow temperature range of 421–446 °C three reactions (E1, P1, U1) take place. The ternary eutectic E1, with the isothermal reaction temperature measured at 423 ± 2 °C, was found to be degenerated concerning to the binary eutectic in the Al-Ge subsystem at 423.7 °C [9]. The eutectic crystallization behaviour was confirmed by very fine microstructures of as-cast samples near to the eutectic point.

A transition reaction, designated as U4, was found to exist in the Al lean part of the phase diagram and ends in the binary eutectic L = Ge + GeNi in the Ge–Ni subsystem. The reaction temperature was found to be 763 ± 3 °C, with a mean value slightly higher than the binary eutectic temperature, given at 762 °C [15]. The composition of the liquid in this reaction is very close to that of the binary eutectic, which was confirmed by the microstructure of a slowly cooled sample with the nominal composition $Al_9Ge_{63}Ni_{28}$, exhibiting definitely the binary eutectic microstructure of Ge + GeNi.

Moreover, a maximum in the three phase field L+(AlNi)+Ge is proposed and the invariant temperature was assessed from the partial liquidus projection at approximately 860 °C. A reaction scheme including all reactions proposed for the Ni-poor part of the system is given in Fig. 7.

Based on the results of all vertical sections as well as primary crystallisation and melting points of several selected samples a partial liquidus projection was drawn (Fig. 8). The projection exhibits three extended primary crystallisation fields of Ge, (Al_3Ni_2) and (AlNi), respectively. One maximum (Max1) is situated in the saddle between the two congruent melting phases Ge and (AlNi). The valleys in the Ni lean part of the projection were found to run very narrow to the binary Al-Ge subsystem due to a very steep increase of the liquidus surface by addition of small amounts of Ni.

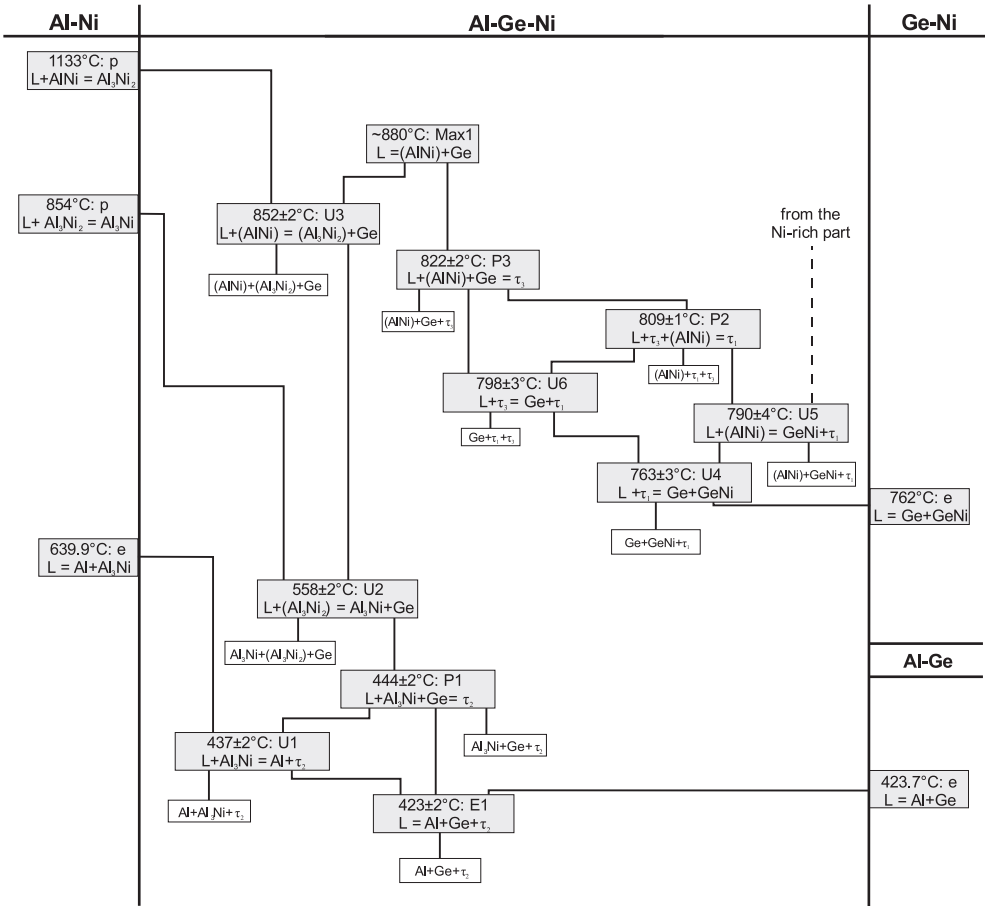

Fig. 7. Partial reaction scheme (Scheil diagram) for the Ni-poor part of the Al–Ge–Ni phase diagram.

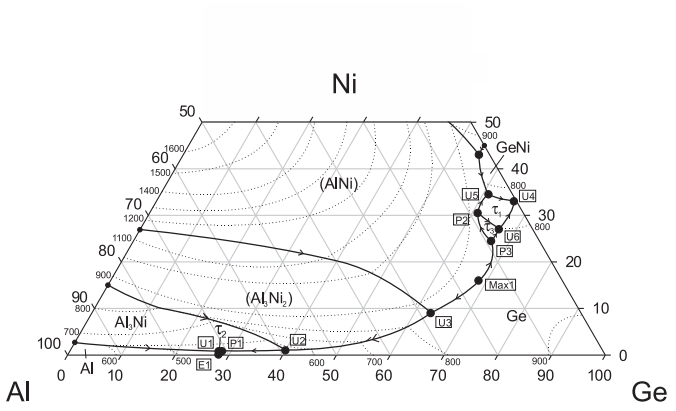

Fig. 8. Partial liquidus surface projection of the ternary Al–Ge–Ni system including the fields of primary crystallization. Solid lines: liquidus valleys. Dotted lines: isotherms. Filled black circles: compositions of liquid at invariant reactions.

τ_2 was found to crystallize only in a very small area, limited by the three invariant ternary reactions E1, P1 and U1. The liquidus valley, joining from the Ni rich part of the phase diagram, was estimated from melting points of respective samples located in this area. There is no information about the Ni rich part of the liquidus projection yet, but phase equilibria and crystallisation behaviour are currently under investigation.

Acknowledgement

The Austrian Science Foundation (FWF) under the project number P 19305 and the "Entwicklungsfonds Seltene Metalle" (ESM) are gratefully acknowledged for financial support. Thomas Reichmann wants to express special gratitude to the Eidgenössischen Materialprüfungs- und Forschungsanstalt (EMPA) for the opportunity of a research stay. Special thanks go also to Dr. Stephan Puchegger, from the Department of Physics/University of Vienna, who provided SEM measurements and Franz Kiraly for his support at EPMA measurements.

Appendix A. Supplementary data

Supplementary data related to this article can be found online at doi:10.1016/j.intermet.2012.04.002.

References

[1] Zielińska M, Yavorska M, Poreba M, Sieniawski J. Thermal properties of cast nickel based superalloys. Archives of Materials Science and Engineering 2010; 44:35–8.
[2] Furrer DU, Fecht HJ. Ni-based superalloys for turbine discs. Journal of Metals 1999;51:14–7.
[3] Sieniawski J. Nickel and titanium alloys in aircraft turbine engines. Advances in Manufacturing Science and Technology 2003;27:23–34.
[4] Jacobson DM, Humpston G. Diffusion brazing. In: Principles of brazing. United states of America: ASM International; 2005. p. 255.
[5] Heinz P, Volek A, Singer RF, Dinkel M, Pyczak F, Göken M, et al. Diffusion brazing of single crystalline nickel base superalloys using boron free nickel base braze alloys, defect and diffusion forum, diffusion in solids and liquids III; 2008. pp. 294–299.
[6] Duvall DS, Owczarski WA, Paulonis DF. TLP bonding. New method for joining heat resistant alloys. Welding Journal 1974;53:203–14.
[7] Nishimoto K, Saida K, Kim D, Nakao Y. Transient liquid phase bonding of Ni-base single crystal superalloy, CMSX-2. ISIJ International 1995;35: 1298–306.
[8] Massalski TB, Okamoto H, Subramanian PR, Kacprzak L. Binary alloy phase Diagrams. 2nd ed. Cleveland: ASM international; 1990.
[9] Srikanth S, Sanyal D, Ramachandrarao P. A re-evaluation of the al-Ge system, Calphad-Computer Coupling of phase diagrams and Thermochemistry, 20; 1996. pp. 321–332.
[10] Minamino Y, Yamane T, Araki H, Adachi T, Kang YS, Miyamoto Y, et al. Isobaric sections of the aluminum phase field in the Al-Ge phase-diagram at high-pressures up to 2.6 Gpa. Journal of Materials Science 1991;26: 5623–30.
[11] McAlister AJ, Murray JL. The Al-Ge (Aluminium-Germanium) system. Bulletin of Alloy Phase Diagrams 1984;5:341–7.
[12] Nash P, Singleton MF, Murray JL. Al-Ni (Aluminium-Nickel). In: Phase diagrams of binary nickel alloys. Cleveland: ASM International; 1991. p. 3–11.
[13] Bitterlich H, Loser W, Schultz L. Reassessment of Ni-Al and Ni-Fe-Al solidus temperatures. Journal of Phase Equilibria 2002;23:301–4.
[14] Okamoto H. Al-Ni (Aluminum-Nickel). Journal of Phase Equilibria 1993;14: 257–9.
[15] Nash A, Nash P. Ge-Ni (Germanium-Nickel). Bulletin of Alloy Phase Diagrams 1987;8:255–64.
[16] Dayer A, Feschotte P. Binary-systems cobalt-germanium and nickel-germanium: a comparative-study. Journal of the Less-Common Metals 1980;72:51–70.
[17] Ellner M, Gödecke T, Schubert K. Zur Struktur der Mischung Nickel-Germanium. Journal of the Less-common Metals 1971;24(4):23–40.
[18] Yanson TI, Zarechnyuk OS, Lushchik GF. Isothermal section through the Ni-Al-Ge system at 770 K. Russian Metallurgy; 1984:238–40.
[19] Ochiai S, Oya Y, Suzuki T. Alloying behaviour of Ni_3Al, Ni_3Ga, Ni_3Si and Ni_3Ge. Bulletin of Research Laboratory of Precision Machinery and Electronics 1983; 32:289–98.
[20] Witt W. Absolute Präzisionsbestimmung von Gitterkonstanten an Germanium- und Aluminium-Einkristallen mit Elektroneninterferenzen. Zeitschrift fuer Naturforschung, Teil A: Astrophysik, Physik und Physikalische Chemie 1967;22:92–5.
[21] Bradley AJ, Taylor A. The crystal structures of Ni_2Al_3 and $NiAl_3$. Philosophical Magazine 1937;23:1049–67.
[22] Nastasi M, Hung LS, Johnson HH, Mayer JW, Williams JM. Phase-transformation of Ni_2Al_3 to NiAl .1. Ion irradiation induced. Journal of Applied Physics 1985;57:1050–4.
[23] Rao PVM, Satyanarayana KM, Suryanarayana SV, Naidu SV. High temperature thermal expansion characteristics of nickel aluminide (Ni_3Al) alloys. Journal of Alloys and Compounds 1993;190:L33–5.
[24] Pfisterer H, Schubert K. Neue Phasen Vom MnP ($B3_1$) – Typ. Zeitschrift Fur Metallkunde 1950;37:112–3.
[25] Straumanis ME, Aka EZ. Lattice parameters, coefficients of thermal expansion, and atomic weights of purest silicon and germanium. Journal of Applied Physics 1952;23:330–4.
[26] Sheldrick GM. A short history of SHELX. Acta Crystallographica Section A: Foundations of Crystallography 2007;64:112–22.
[27] Eslami H, Francheschi JD, Gambino M. An electromotive force study of the activity of aluminum in aluminum-gallium, aluminum-germanium and aluminum-gallium-germanium systems. Zeitschrift fuer Naturforschung 1979;34A:810–7.
[28] Richter KW, Ipser H. The Al–Ni–Si phase diagram between 0 and 33.3 at.% Ni. Intermetallics 2003;11:101–9.
[29] Takizawa H, Uheda K, Endo T. $NiGe_2$: a new intermetallic compound synthesized under high-pressure. Journal of Alloys and Compounds 2000;305: 306–10.